ORIGINAL RESEARCH

Outer Membrane Vesicles Coating Nano-Glycyrrhizic Acid Confers Protection Against *Borderella bronchiseptica* Through Th1/Th2/Th17 Responses

Yee Huang [iD], Li Nan, Chenwen Xiao, Jie Dong, Ke Li, Jvfen Cheng, Quanan Ji, Qiang Wei, Guolian Bao, Yan Liu

Institute of Animal Husbandry and Veterinary Medicine, Zhejiang Academy of Agricultural Science, Hangzhou, 310021, People's Republic of China

Correspondence: Guolian Bao; Yan Liu, Institute of Animal Husbandry and Veterinary Medicine, Zhejiang Academy of Agricultural Science, Hangzhou, 310021, People's Republic of China, Email baoguolian@163.com; 35792191@qq.com

Purpose: Outer membrane vesicles (OMVs) are spherical nano-sized proteolipids secreted by numerous pathogenic Gram-negative bacteria. Due to the immunostimulatory properties and protective efficacy, OMVs have received increasing attention as a candidate for the vaccine to prevent and treat bacterial infections. However, the immune response remains elusive due to the low structural stability and poor size homogeneity of the vesicles. In this study, OMVs were used to coat self-assembled glycyrrhizic acid nanoparticles (GANs) and obtain a stable OMV vaccine. The immunoprotective effects and anti-infection efficacy were evaluated in vivo and in vitro.

Methods: The OMVs were prepared by ultrafiltration method and fused with GAN through mechanical extrusion. The characteristics, including morphology, hydrodynamic size, zeta potential, and stability were evaluated. The in vitro immunological function of GAN-OMV on the macrophages and in vivo immune efficacy and anti-infection effect were examined and compared.

Results: The results showed that the GAN-OMV were homogenous with a size of 130 nm and a stable core-shell structure. Micropinocytosis-dependent and clathrin-mediated endocytotic pathways effectively internalized the GAN-OMV into the macrophages and promoted cell proliferation, cytokine secretion, and M1 polarization. Furthermore, subcutaneous GAN-OMV vaccination contributed to significantly higher *Borderella bronchiseptica* (Bb)-specific antibody production and lymphocyte proliferation. The splenic lymphocytes of mice immunized with GAN-OMVs displayed a higher ratio of CD4+/CD8+ T cells and CD19+ B cells and produced significantly higher levels of Th1/Th2/Th17 cytokines. GAN-OMV also effectively prevented Bb reinfection.

Conclusion: In this study, GAN-OMV was developed successfully to stimulate Th1/Th2/Th17 immune responses against Bb and provide a promising strategy for novel vaccine development against the microbial pathogen.

Keywords: outer membrane vesicles, glycyrrhizic acid nanoparticle, macrophage, protective immune response, anti-bacterial infection

Introduction

In recent years, a huge burden of infectious diseases has been experienced globally despite advances in medicine. With the advent of the post-antibiotic era, antimicrobial vaccines are an urgent requirement. Outer membrane vesicles (OMVs) have received increasing attention as a promising new approach for vaccine development against bacterial pathogens.[1] OMV is a non-replicative, nanosized (10–300 nm diameter), spherical, bilayered proteolipid, naturally released during the growth of Gram-negative bacteria.[2,3] It is primarily comprised of bacterial outer membrane constituents, contains the main immunogenic antigens of the parent bacteria, and exhibits various pathogen-associated molecular patterns required to elicit innate immunity and promote adaptive immune responses.[4] Due to the immunostimulatory properties and

proteoliposome nanostructures, OMV has been increasingly explored as an ideal vaccine or delivery system for preventing and treating bacterial infections.

With the development of nanotechnology, combining synthetic nanoparticles with natural cellular materials has generated various biomimetic nanoparticles.[5–7] The synthetic nanoparticles can be appropriately tuned to maximize the immunization effect of vaccines. Therefore, the OMV-coating nanoparticle vaccines combine the advantages of OMV vaccines and nanoparticles and would elicit a stronger antigen-specific immune response. Based on the technological advances, this study aimed to utilize OMVs to coat gycyrrhizic acid (GA) self-assembled nanoparticles and investigate their potential as anti-bacterial vaccines.

GA is a main bioactive compound extracted from the licorice and has been widely used as a traditional Chinese medicinal herb. It exhibits several pharmacological features, including immunomodulating, antioxidative, antiulcerative, antimicrobial, antiviral and anti-tumor properties.[8–10] In the current study, the immunomodulatory role of GA was excavated as a potential adjuvant agent. However, the therapeutic potential of GA is limited due to its poor solubility in biological fluids, resulting in its low bioavailability.[11]

The self-assembly of small molecules, especially naturally occurring molecules, could benefit bioavailability, biocompatibility, and biodegradability.[12] GA is an amphiphilic molecule containing a hydrophilic (two glucuronide residues) and a hydrophobic (aglycone) portion and thus can self-associate in aqueous media.[13] In this study, GA was prepared into nano-formulation and encapsulated with OMV (Figure 1).

In this study, we used the coating of OMV on the surfaces of self-assembled GA nanoparticles (GANs) to combine the merits of two distinct materials and generate strong anti-bacterial immune responses. OMV preserve the biological characteristics of their parent bacteria and mimic their natural antigen presentation to the immune system. Moreover, the GAN core is beneficial for maintaining OMV stability and effective antigen presentation to the immune cells.
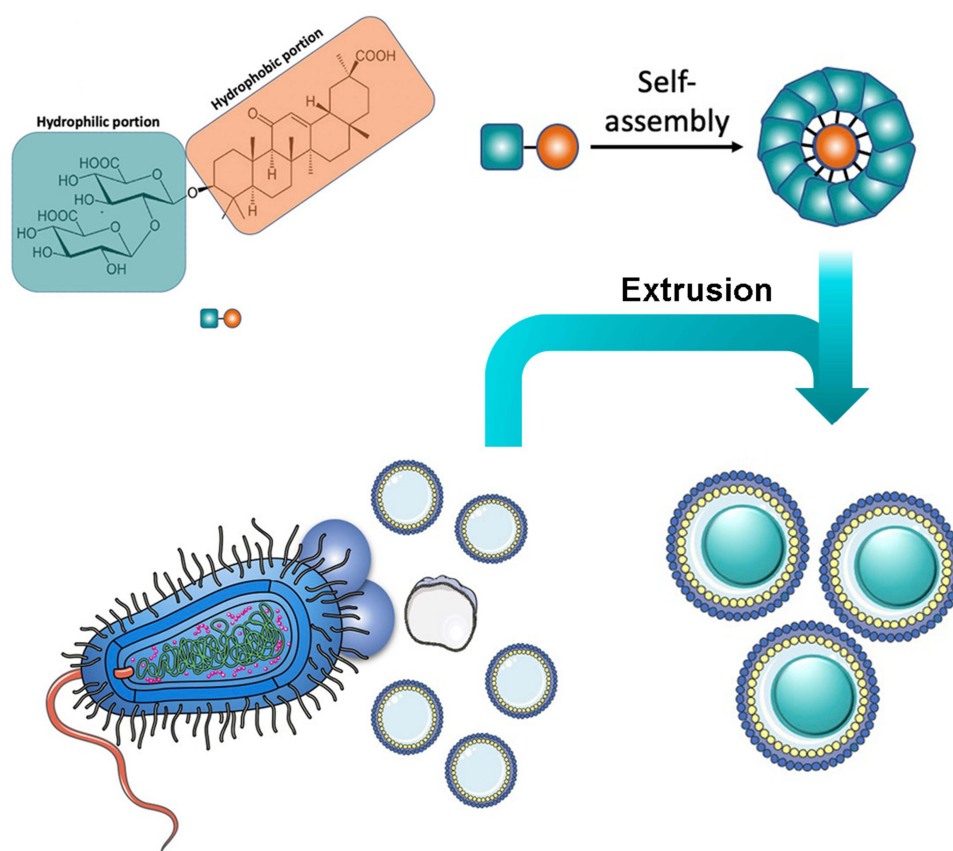
Figure 1 Chemical structure of GA and schematic of OMV coating on GA nanoparticles.

Herein, we chose *Bordetella bronchiseptica* (Bb) as a model pathogen, which is the cause of infectious respiratory disease in dogs, atrophic rhinitis in pigs, snuffles in rabbits, and pneumonia in immuno-compromised individuals.[14,15] In addition, the effects of GAN-OMV were preliminarily investigated on the immunological function of macrophages and compared to that of the single OMV. Following the in vitro experiments, GAN-OMV was subcutaneously injected into mice, which subsequently elicited a mixed Th1/Th2/Th17 response in the vaccinated animals. Collectively, this study provided a promising approach for developing an anti-bacterial vaccine.

Materials and Methods
Materials

Bordetella bronchiseptica (*Bb*) strain FX used in this study was isolated from a rabbit farm in Zhejiang Province with infectious rhinitis and maintained in our laboratory. GA (with a purity of UV 95%, molecular weight: 822.93) was purchased from Shanghai Yuanye Bio-Technology Co. Ltd. Alum adjuvant was purchased from Thermo scientific. Dulbecco's modified Eagle's medium (DMEM) (Gibco) was supplemented with 10% fetal bovine serum (FBS, Gibco), penicillin (50 units/mL) and streptomycin (50 μg/mL). Cell counting kit-8 (CCK-8) was purchased from Biosharp. Lipopolysaccharide (LPS) was obtained from Sigma Aldrich (St. Louis, MO, USA). Endocytosis inhibitors including chlorpromazine, cytochalasin D or filipin were obtained from Sigma-Aldrich.

Bacteria Culture and Generation of Bacterial OMV

Bb strain FX was grown routinely on tryptone soya ager (TSA) (Thermo) at 37 °C for 36 h. Then, a single colony was inoculated into tryptone soya broth (TSB) (Thermo). Following inoculation, the bacteria were cultured in a rotary shaker at 37 °C for 10 h, and then refreshed with TSB enriched with 64 μg/mL cefalexin at a 1:100 dilution, followed by continued growth for 18 h. OMVs were prepared according to our previous study.[16] Briefly, the bacteria were collected by centrifugation of 1 L culture medium at 10,000g for 20 min, followed by filtering through a 0.45-μm pore membrane. The filtrate was then concentrated using a filter membrane with a molecular weight cutoff (MWCO) of 100 kDa. The concentrated medium was further clarified by centrifugation at 100,000g, 4 °C for 2 h. The OMV pellet was resuspended in the 1X sterile phosphate-buffered saline (PBS) and filtered using 0.22-μm pore membrane (Millipore) to avoid contamination of bacteria or cell debris. Notably, all the preparation processes were conducted under sterile conditions to avoid contamination. All the samples were stored at −80 °C for subsequent experiments.

Preparation of GAN and GAN-OMV

For GAN preparation, methanol-esterified GA was solubilized in methanol and ethyl acetate (v:v-1:1). The mixture was emulsified by ultrasonication with DSPE-PEG2K and stirring overnight to evaporate the organic solvent and obtain GAN, which was stored at 4 °C. In some experiment, GAN need to label with FITC. In this case, DSPE-PEG2K was replaced with DSPE-PEG2K-FITC.

Subsequently, it was homogenized with ultrasound by an Ultrasonics Vibracell probe sonicator. Then, a mechanical extrusion process was employed to synthesize GAN-OMV by mixing GAN and OMV at a 1:1 volume ratio and sterilizing by filtration through a 200-nm filter membrane. Subsequently, the mixture was subjected to 10-circle extrusion by an Avanti extruder to yield the final GAN-OMV formulation.

In some experiment, OMVs were labeled with DiI. OMVs were incubated with 1 μM DiI (Vybrant DiI Cell-labeling solution) for 30 min at 37 °C. Excess DiI was removed by ultracentrifugation at 150,000g for 3 h at 4 °C.

OMV, GAN, and GAN-OMV Characterizations

Protein concentration was determined using the Bradford Protein Assay Kit (Solarbio). For transmission electron microscope (TEM) imaging, OMV, GAN, and GAN-OMV were placed on 200 mesh copper grids and stained with 2% phosphotungstic acid, respectively. Images were obtained using H7650 TEM (Hitachi) at 80 kV. The size and zeta potential of OMV, GAN, and GAN-OMV were measured by dynamic light scattering (DLS) using Malvern Zetasizer

(ZS90, UK). To assess the stability of GAN-OMV, samples were maintained at 4 °C, and the diameter and zeta potential of GAN-OMV were detected by DLS at the indicated time points in triplicate.

Cell Proliferation Experiments

RAW264.7 murine macrophages were obtained from the Chinese Academy of Science Cell bank (Shanghai, China) and cultured in DMEM containing 10% FBS, 100 μg/mL penicillin, and 100 μg/mL streptomycin. The cells were seeded in 96-well plate at a density of 5×10^3 cells/well and incubated at 37 °C, 5% CO_2 for 24 h. Subsequently, the complete medium containing predetermined concentrations of either GAN-OMV, GAN, or OMV was added. The final concentration of GAN was 200, 100, 50, 25 and 12.5 μg/mL, and the final concentration of OMV was 60, 30, 15, 7.5 and 3.75 μg/mL. LPS was a positive control, while medium alone was the negative control (BC). The culture was continued for an additional 24 h. Then, CCK-8 reagent was added to each well and further incubated for some time. The absorbance was measured at 450 nm.

To determine the endocytic pathway for GAN-OMV internalization into RAW264.7 cells, various endocytosis inhibitors were applied. Macrophages were plated at a density of 5000 cells/well in 96-well plates in complete medium for 24 h. Then, the cells were then washed with D-Hank's, followed by preincubation with one of the following endocytosis inhibitors solubilized in serum-free DMEM [chlorpromazine (an endocytotic inhibitor of clathrin-mediated endocytosis), cytochalasin D (an endocytotic inhibitor of micropinocytosis-mediated endocytosis), or filipin (an endocytotic inhibitor of caveolae-dependent endocytosis)] at 37 °C for 1 h. Next, the medium was replaced with complete DMEM containing drugs at various concentrations and different inhibitors for another 24 h. The cell proliferation was evaluated using the CCK-8 assay.

Cytokine Assays

RAW264.7 cells were cultured as described above for cytokine assays. After 24-h co-culture with different drugs, the cell supernatant was collected, and tumor necrosis factor-alpha (TNF-α), interleukin (IL)-1β, IL-10, and IL-6 levels were measured using enzyme-linked immunosorbent assay (ELISA) kits (Multi Sciences), according to the manufacturer's instructions, on a BioTek Synergy HT microplate reader.

Cell Internalization Tests

Cell internalization tests were conducted as described previously.[17] RAW264.7 cells were cultured as described above. Briefly, the cells were inoculated in 6-well plate at a density of 10^5 cells/well and incubated in a complete medium for 24 h. Then, the cells were washed with D-Hank's twice, followed by preincubation at 37 °C with one of the following endocytosis inhibitors dissolved in serum-free DMEM: chlorpromazine, cytochalasin D, or fillpin.[18] Next, the medium was replaced with complete DMEM containing fluorescent dyes-labeled GAN-OMV (OMV was labeled with DiI and GAN was labeled with FITC) and various endocytosis inhibitors for an additional 4 h. To determine the endocytic pathway through which GAN-OMV is internalized into RAW264.7 cells, the slides were observed under a confocal laser scanning microscope (Leica).

In order to determine the subcellular distribution of OMV, RAW264.7 cells were cultured as described above. Briefly, 10^5 cells/well were inoculated in 6-well plate in the complete medium for 24 h. Each well of the 6-well plate was pre-placed with glass slides, which facilitate to observe under microscope. After treatment with DiI-labeled OMV for 3.5 h, the cell supernatant was discarded, and the lysosomes were stained with LysoTracker-green (Invitrogen). The slides were taken out and observed under a confocal laser scanning microscope (Leica).

Generation and Polarization Bone Marrow-Derived Macrophages (BMDMs)

To determine the effect of GAN-OMV on macrophage polarization, BMDMs were isolated from BALB/c mice by flushing tibiae and femurs through a 40-μM cell strainer with cold PBS (Sigma–Aldrich). Then, the red blood cells (RBCs) were lysed with Tris-buffered ammonium chloride, neutralized, suspended in DMEM supplemented with 10% FBS, 100 μg/mL penicillin, and 100 μg/mL streptomycin, and seeded in 6-well plates at a density of 1.5×10^6 cells/well. To generate macrophages, 10 ng/mL murine M-CSF (Peprotech, Rocky Hill, NJ, USA) was added to the cultures and

placed in a 37 °C, 5% CO_2 humidified atmosphere for 4 days (M_0). BMDMs were further cultured for 2 days in fresh medium (containing 10 ng/mL M-CSF) supplemented with GAN-OMV (GA: 10 μg/mL, OMV: 3 μg/mL). For M1 stimulation, the medium was supplemented with 10 μg/mL LPS and 20 ng/mL murine interferon-gamma (IFN-γ), while for M2 stimulation, it was supplemented with 20 ng/mL murine IL-4 and 20 ng/mL murine IL-10 (Peprotech).

After incubation, the BMDMs were collected and washed, followed by flow cytometry to evaluate the expression of CD11b, CD80, and CD206 using a FACSCanto™ II flow cytometer (BD Biosciences, San Jose, CA, USA).

Animals and Immunization

All animal experiments were approved by the Animal Welfare and Ethics Committee of Zhejiang Academy of Agricultural Sciences (Ethics protocol no. 1935) in accordance with the Chinese guidelines for the care and use of laboratory animals. The studies were conducted following the principles and guidelines of the Farm Animal Welfare Council of Zhejiang, China. Female BALB/c mice, aged 6-weeks-old, were purchased from Hangzhou Ziyuan Laboratory and acclimatized to standard environment conditions (temperature=23±2 °C; humidity=55±10%) for 1 week before immunization and allowed free access to standard laboratory animal diet and water *ad libitum*.

The groups of mice were immunized three times (days 0, 7, and 14) subcutaneously with 200 μL GAN-OMV (containing 1 μg OMVs and 100 μg GAN), a mixture containing 1 μg OMVs/alum (positive control), 1 μg OMVs, or PBS (negative control).

Antigen-Specific IgG, IgG1, or IgG2a Determination by ELISA

Serum samples were obtained from peripheral blood withdrawn from each mouse on day 42 for analysis of antibody and cytokines (n=6/group). After coagulation (60 min, 37 °C), sera were collected by centrifugation (15 min, 3000 rpm) and stored at −80 °C until use. ELISA was used to assay the antibody titers against OMV or Bb whole-cell lysates in sera.[19] OMV and the whole protein (10 μg/mL and 2 μg/mL) from Bb bacteria were dissolved in 0.05 M carbonate buffer, respectively. The resulting protein solution (100 μL/mL) was used to coat the 96-well plates (Corning) and incubated at 37 °C, overnight. Subsequently, the plates were washed four times with PBST, followed by blocking with 5% non-fat milk-PBS at 37 °C for 2 h. After three washes, 100 μL of the diluted serum sample (1:10) was added to each well. The plates were then incubated at 37 °C in the dark for 1 h. Next, horseradish peroxidase-conjugated goat anti-mouse IgG, IgG1, and IgG2a (Abcam) were added to each well, respectively, and incubated at 37 °C for 1 h. Finally, ELISA TMB (ready-to-use) (Multi Sciences) was added, and after incubation at 37 °C in the dark for 15 min, the reaction was stopped with 100 μL/well of stop reagent (0.5 M H_2SO_4). The absorbance was measured at 450 nm on a microplate reader.

Splenocyte Proliferation Assay

Spleens were obtained aseptically from euthanized mice (n=6/group) on day 42 and dissociated using a cell strainer and a sterile plunger from a 5-mL syringe. RBCs were lysed and an equivalent of $5×10^6$ cells was plated in 96-well cell culture plates and stimulated in vitro for 72 h with Con A, LPS, and OMV. The CCK-8 method was used to measure cell proliferation. The data were expressed as the proliferation index, calculated based on the following formula:

Proliferation index=OD (450 nm) for stimulated cultures/OD (450 nm) for non-stimulated cultures.

Evaluation of Lymphocyte Activation and T Cell Response

As described above, splenocytes from mice (n=6/group) were harvested on day 42. Next, splenocytes were collected, washed, and stained with anti-CD3-FITC, anti-CD4-PerCP, and anti-CD8-APC or anti-CD19-PE (Multi Sciences) at 4 °C for 30 min. The cells were assessed on a BD FACS ARYA III flow cytometer. The control group for gating was stained with anti-CD3-FITC, anti-CD4-PerCP, and anti-CD8-APC or anti-CD19-PE, respectively. The percentage of CD4 T cells (CD3+CD4+) and CD8 T cells (CD3+CD8+) was analyzed after selecting CD3-positive cells, and the percentage of CD19+ cells was analyzed based on the positive content. The percentage of activated lymphocytes (CD19+), CD4 T cells (CD3+CD4+), and CD8 T cells (CD3+CD8+) were further analyzed using FlowJo software, which represented the effect of GAN-OMV on lymphocyte activation and T cell response.

Cytokine Expression in Restimulated Splenocytes and Serum

As described above, splenocytes from mice (n=6/group) were harvested on day 42. The single-cell suspension obtained from the spleen was stimulated for 3 days with OMV (5 μg) to induce cytokine production. Then, the supernatant was collected, and the concentration of T-helper-related cytokines, interleukin-4 (IL-4), IL-6, TNF-α, and IFN-γ, was determined using the corresponding ELISA kits.

The presence of IL-4 and IFN-γ in the serum samples was determined using the mouse ELISA kits (Multi Sciences) in accordance with the manufacturer's instructions.

Complement-Mediated Bactericidal Assay

The bactericidal activity of the serum collected from mice on day 28 was tested in vitro. Briefly, Bb was grown on TSA medium and diluted to 1×10^3 colony-forming unit (CFU)/mL in PBS. Both immune and naïve sera were heat-inactivated at 56 °C for 30 min prior to use. Guinea pig complement was selected for its absence of bactericidal activity against the test strains (Figure S1). The serum samples were serially diluted two-fold in a 96-well plate, and 40 μL of diluted test serum was mixed with 20 μL of guinea pig complement and 20 μL of the bacterial suspension. The mixture of bacteria in PBS without guinea pig complement or without serum was used as controls. Then, the 96-well plates were sealed and incubated on a shaker incubator (100 rpm) at 37 °C for 1 h. Subsequently, 50 μL of each mixture was plated on TSA medium, incubated for 24 h, and the colonies were counted on a colony counter (Scan 1200, Interscience). The data were expressed as a bactericidal rate, calculated based on the following formula:

$$\text{Bactericidal rate (\%)} = (\text{colonies}_{\text{naive sera}} - \text{colonies}_{\text{immune sera}}) / \text{colonies}_{\text{naive sera}} \times 100\%$$

Challenge Assay

To confirm the protective effect of vaccination against bacterial infection, Bb was challenged with the FX strain (6×10^6 CFU) of immunized and naive mice (n=6/group) on day 28. Then, the mice were sacrificed by cervical dislocation on day 7 post-challenge. The lungs for colonization assays were homogenized in 2 mL TBS using a bullet blender at 60 Hz for 3 min. Serial dilutions (1:10, 1:100, and 1:1000) of each lung homogenate were plated on TSA, and each count was confirmed using a colony counter to determine the number of Bb inside the lungs.

Statistical Analysis

All values are expressed as means±standard error (SE). The statistically significant differences between groups were determined using one-way or two-way analysis of variance (ANOVA) following Tukey's or Bonferroni post-hoc comparison. Student's *t*-test analysis was performed using GraphPad Prism software (Version 8, San Diego, CA, USA). *$P<0.05$, **$P<0.01$, ***$P<0.001$, ****$P<0.0001$ indicated significant differences.

Results

Characterization of OMV Derived from *Bb* and Its Combination with GAN

In this study, GAN was functionalized with OMV for improved subunit vaccine performance. The OMV was obtained from the supernatant of Bb and fused onto the surfaces of GAN.

The electron microscopy analysis of OMV suggested a bilayer structure and a uniform circular morphology of the vesicle with a diameter of ~300 nm. The combined GAN-OMV exhibited an obvious core-shell structure (Figure 2A).

As shown in Figure 2, the average size of GAN was 104±1.66 nm. After OMV was fused with GAN, the average size of GAN-OMV was increased to 130.43±9.73 nm. The zeta potential of GAN, OMV, and GAN-OMV was −21.77±0.95 mV, −22.95±1.34 mV, and −30.4±1.31 mV, respectively (Figure 2B, Figure S2). GAN-OMV showed good stability within 21 days, and the size and zeta potential only showed a slight increase (Figure 2E).
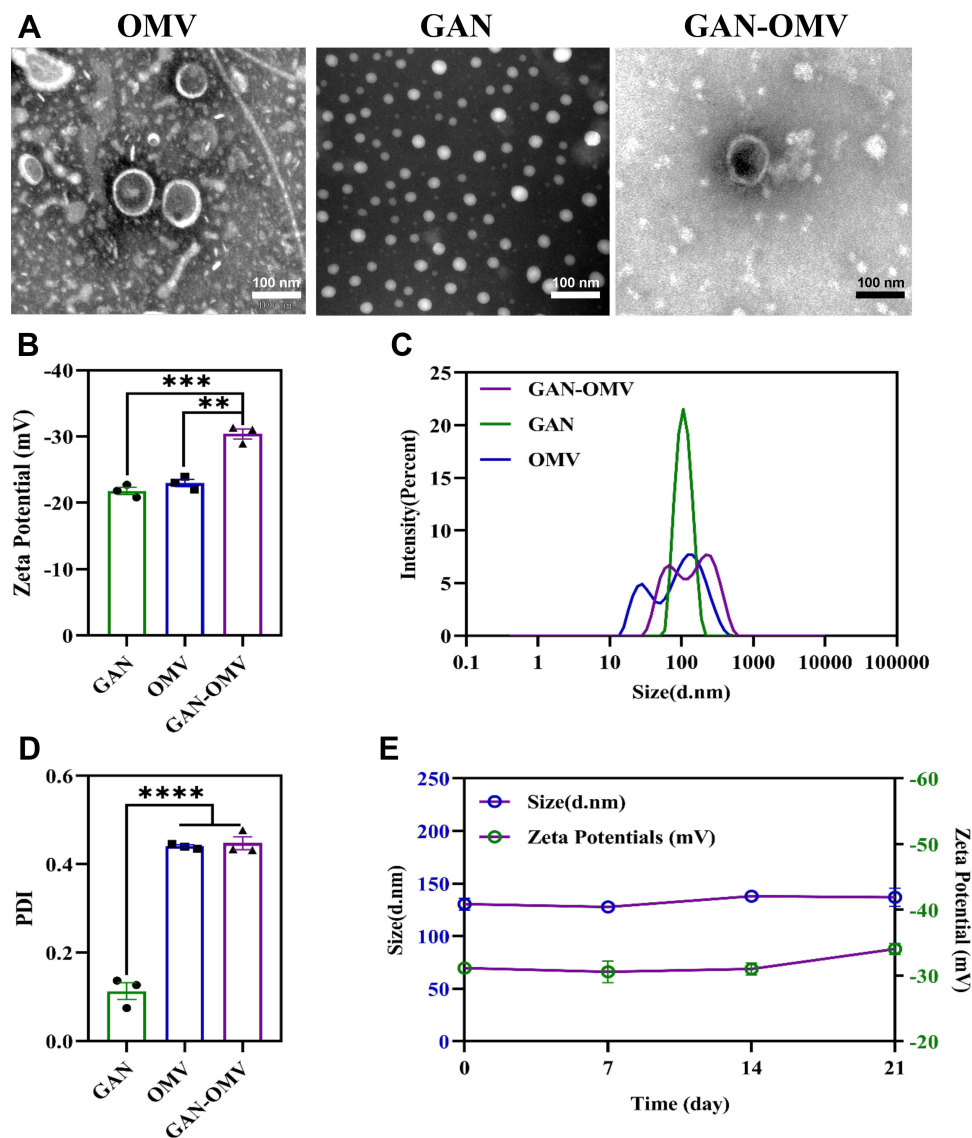
Figure 2 Characterization of OMV, GAN, and GAN-OMV. (**A**) TEM image; (**B**) Zeta potential; (**C**) Size distribution; (**D**) PDI value of OMV, GAN, and GAN-OMV; (**E**) Stability of GAN-OMV. (Bar=200 nm, **P<0.01, ***P<0.001, ****P <0.00001).

## GAN-OMV Exhibited Better Effects on Macrophage Proliferation and Its Cytokine Production Over Single OMV

Macrophages comprise the first line of host immune defense, which serves antigen-presenting cells (APCs) and modulates the adaptive immune response.[20] Mouse mononuclear macrophages RAW264.7 cells, comprise the commonly used cell model to investigate the immunoregulatory activities of natural compounds.[21] In this study, the effects on RAW264.7 proliferation were investigated using the CCK-8 assay. The results showed that GAN-OMV promotes macrophage proliferation in a range of 3.75–60 μg/mL in a dose-dependent manner. As shown in Figure 3A, the OD_{450nm} value was significantly higher than that of single OMV and GAN at the same concentration (P < 0.05).

Promoting APCs secretion of pro-inflammatory cytokines is required for potent adaptive immune responses.[22] IL-1β, TNF-α, IL-6, and IL-10 levels were tested in the macrophage supernatant after co-cultured with GAN-OMV, OMV, and GAN, respectively. The current results showed that GAN-OMV significantly increased cytokines production, which is higher than that of single OMV and GAN at the same concentration (Figure 3B–E).
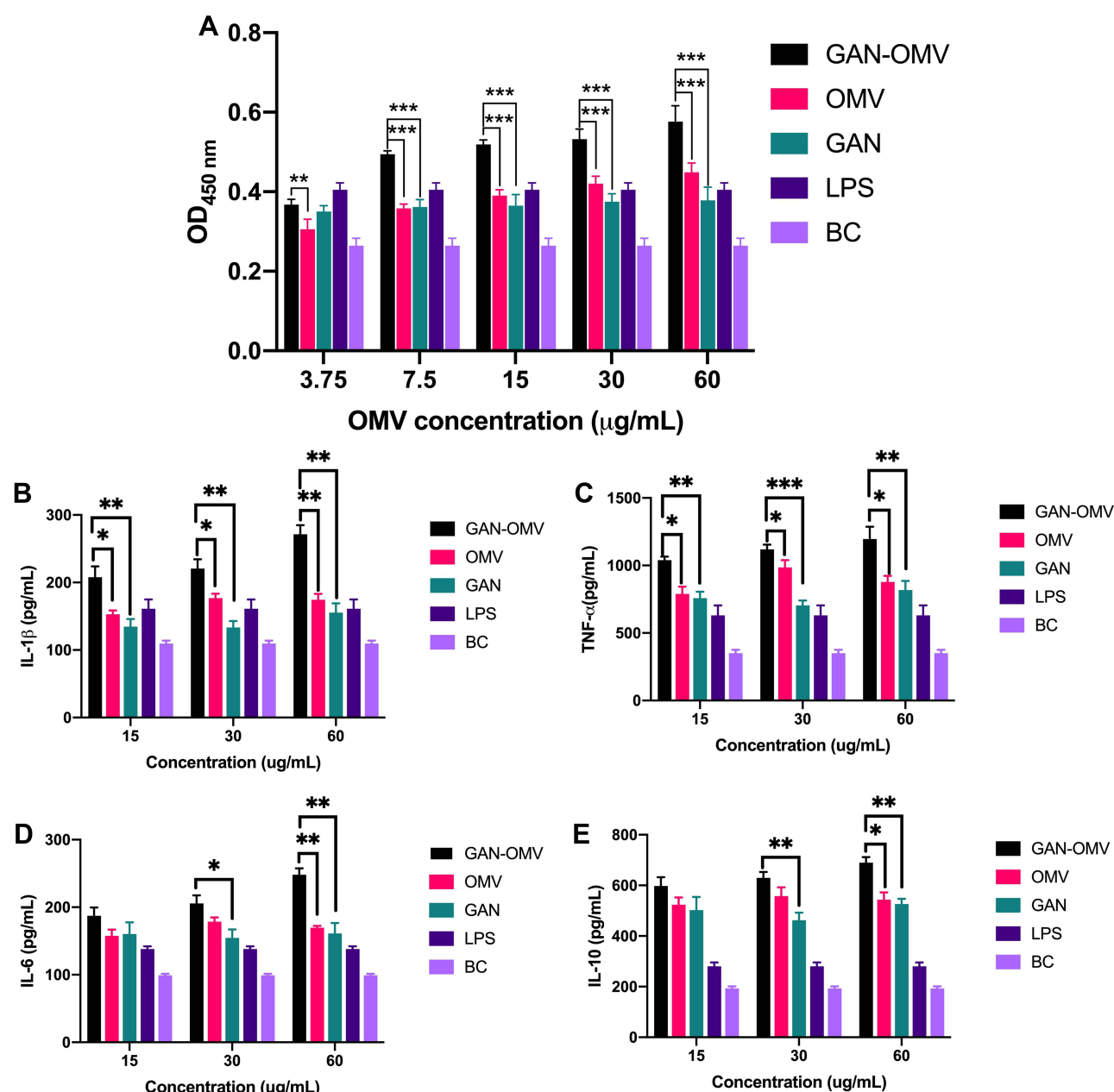
Figure 3 Cell viability of RAW264.7 cells in the stimulation of GAN-OMV, OMV, and GAN at 450nm (**A**). LPS was the positive control, and the BC was the negative control. The effects of GAN-OMV on the secretion of IL-1β, TNF-α, IL-6, and IL-10 (**B–E**). (*P<0.05, **P<0.01, ***P<0.001).

Macrophages are classified into two phenotypically distinct groups: the pro-inflammatory M1 type (classically activated macrophages) and the anti-inflammatory M2 type (alternatively activated macrophages). The M1 macrophages release proinflammatory cytokines, such as TNF-α, IL-12, and IL-6, to activate the immune system. Conversely, the M2 macrophages release anti-inflammatory cytokines, such as IL-10 and transforming growth factor-beta (TGF-β).[23,24] Previous studies showed that M1 macrophages are CD80^{hi}CD206^{lo}, while M2 macrophages are CD80^{lo}CD206^{hi}.[23,25] The present results demonstrated a significantly increased expression ratio of CD80/CD206 in GAN-OMV than that in OMV, indicating that GAN-OMV induces an efficient M1 polarization (Figure 4).
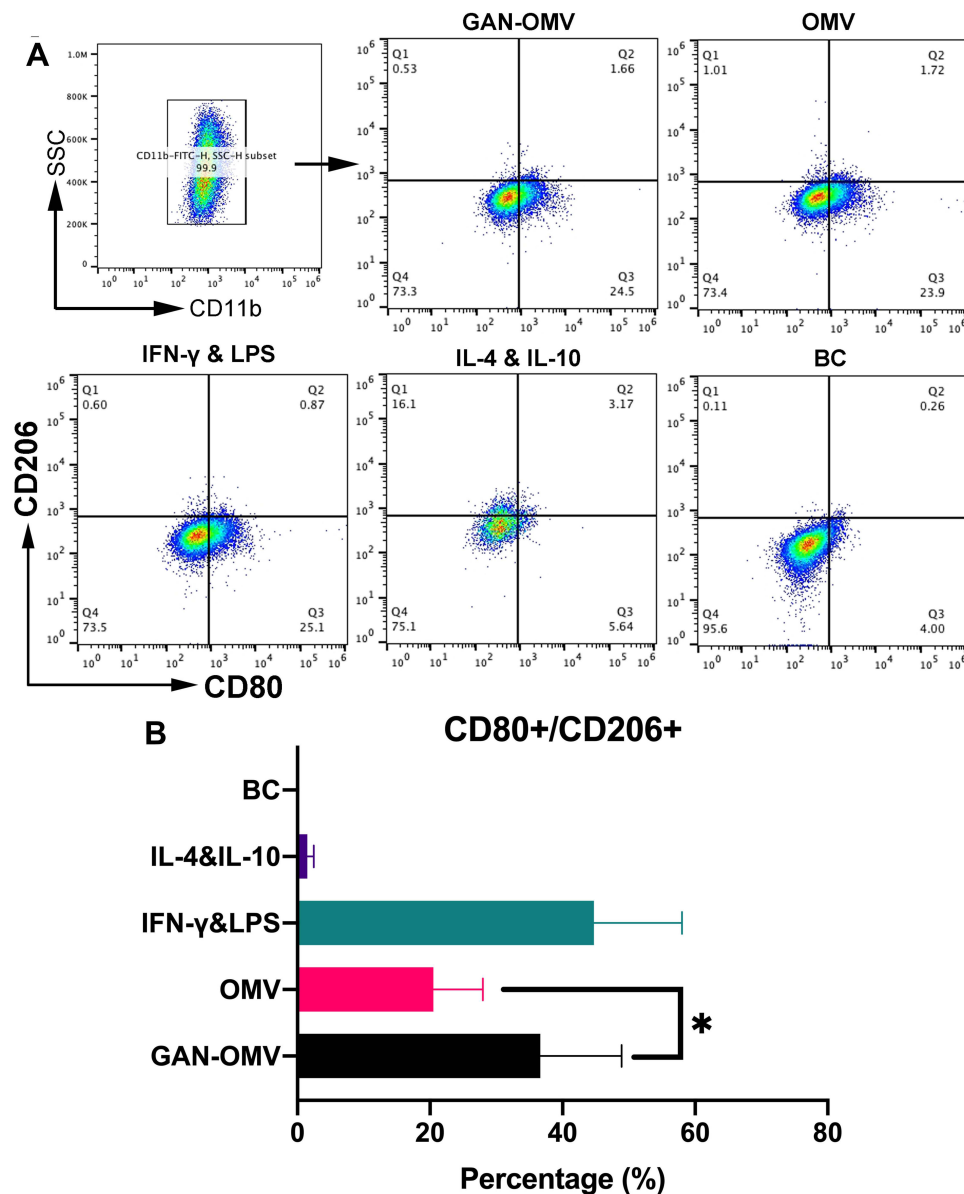
Figure 4 Effect of GAN-OMV on the macrophage polarization. (**A**) Flow cytometry of BMDMs stimulated with GAN-OMV, OMV, LPS/IFN-γ (M1), or IL-4/10 (M2). CD11b^{+} populations are marked within rectangles. Then CD80^{+}CD206^{−} and CD80^{−}CD206^{+} populations were gated. (**B**) Quantitative analysis of the ratio of CD80^{+}/CD206^{+}. Statistical analysis was performed with one-way ANOVA. *$P<0.05$.

GAN-OMV Internalized into Macrophages Through Micropinocytosis-Dependent and Clathrin-Mediated Endocytosis Pathways

Vaccine internalization by APCs, especially DCs and macrophages, is critical for immune activation.[26] To assess the ability of the synthesized nanoparticles to be taken up by macrophages and the pathway(s) through which these are internalized into the cells, we incubated RAW264.7 with GAN-OMV. Under the confocal microscope, the GAN-OMV internalization level was decreased significantly after chlorpromazine (an endocytotic inhibitor of clathrin-mediated endocytosis) and cytochalasin D (an endocytotic inhibitor of macropinocytosis-mediated endocytosis) treatment. Moreover, GAN-OMV also entered the macrophages treated with filipin (an inhibitor of caveolae-mediated endocytosis) and did not differ significantly from the cells without any inhibitors (Figure 5A).

To further confirm these results, the proliferation level before and after treatment with the inhibitors was compared. Based on these results, the proliferation level of RAW264.7 was significantly decreased after pretreatment with
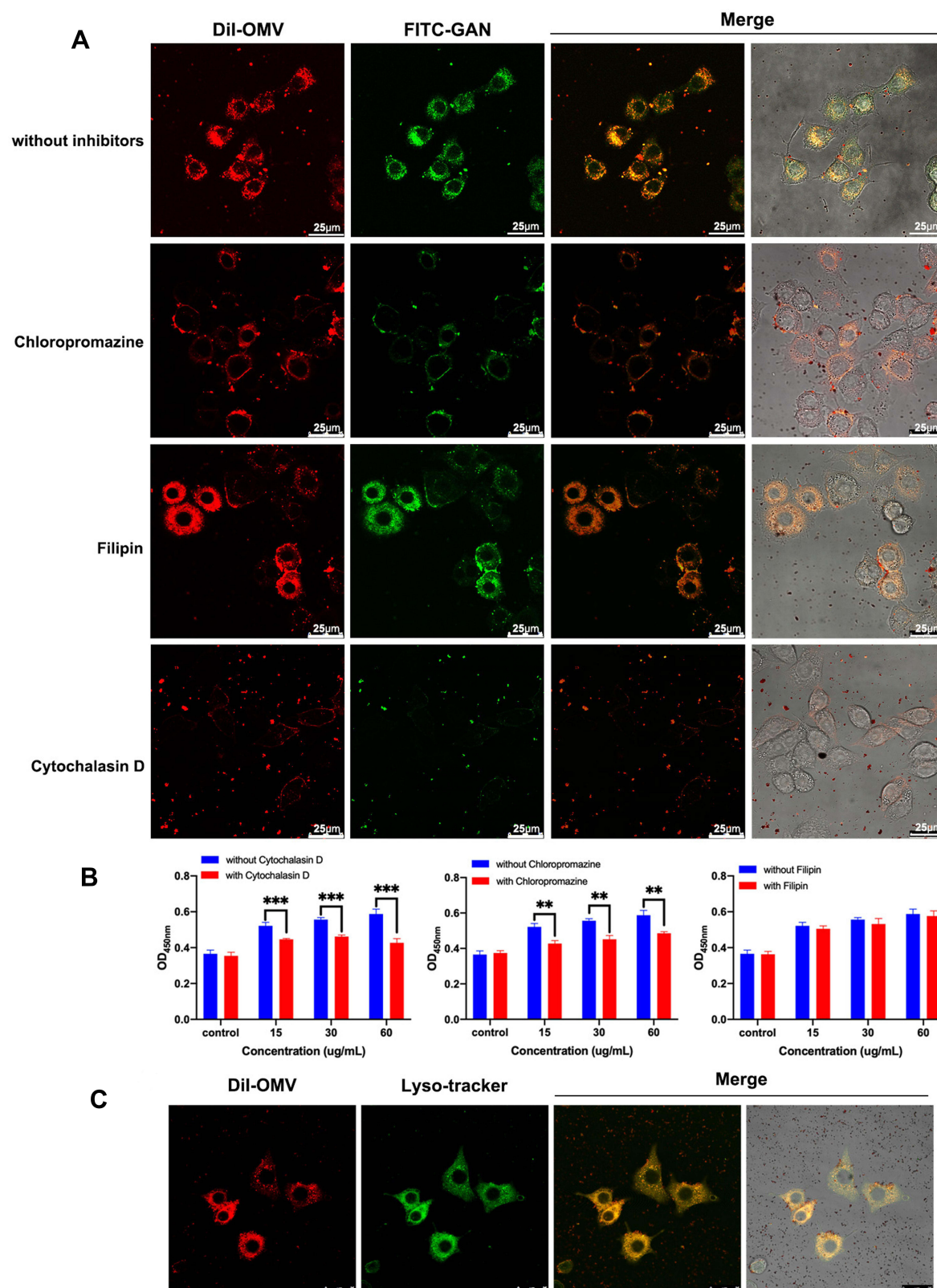
Figure 5 GAN-OMV internalized macrophages via different endocytic pathways. (**A**) RAW264.7 cells were pretreated with chlorpromazine (an endocytotic inhibitor of clathrin-mediated endocytosis), cytochalasin D (an endocytotic inhibitor of macropinocytosis-mediated endocytosis) or fillipin (an inhibitor of caveolae-mediated endocytosis). The intracellular uptake of GAN-OMV was investigated under confocal microscopy. (**B**) Changes of cell viability of RAW264.7 cells by cytochalasin D, chlorpromazine, and filipin were measured by CCK-8 method. **$P < 0.01$, ***$P < 0.001$. (**C**) Intracellular distribution of GAN-OMV was observed under confocal microscopy.

cytochalasin D and chlorpromazine, while no difference was detected in the filipin-treated cells (Figure 5B). Both the results indicated that GAN-OMV enters macrophages through micropinocytosis-dependent and clathrin-mediated endocytotic pathways.

To investigate the cellular uptake of GAN-OMV, we labeled OMV and conjugated it with GAN. After 2 h treatment, GAN-OMV showed a substantial intracellular accumulation. The red fluorescence was co-localized with green lyso-tracker, used to label the lysosomes inside the cells (Figure 5C).

These findings conclusively demonstrated that micropinocytosis-dependent and clathrin-mediated endocytic pathways were the main pathways through which GAN-OMV was internalized into macrophages and promoted cell proliferation and cytokine production.

GAN-OMV Induced Antigen-Specific Antibodies

GAN-OMV was shown to accumulate in the macrophages, increasing their proliferation, cytokine secretion, and M1 polarization in vitro. Subsequently, the ability of our nanovaccine to generate antigen-specific immune responses in vivo was examined. Thus, mice were immunized three times with different OMV formulations: GAN-OMV, OMV, alum-OMV, and PBS (blank control). Anti-OMV and anti-Bb antibody levels were measured 4 weeks after the last immunization. As shown in Figure 6A, both GAN-OMV and alum-OMV induce significantly high levels of OMV-specific IgG, IgG1, and IgG2a, which were significantly higher than that of OMV group. However, no significant difference was detected between GAN-OMV and alum-OMV. To further confirm whether OMV-immunized mice could generate a strong immune response against Bb, Bb-specific IgG, IgG1, and IgG2a were evaluated (Figure 6B). Based on these results, after three vaccinations in 7-day intervals, the levels of Bb-specific antibodies increased in the GAN-OMV immunized mice, which were significantly higher than that in OMV-immunized mice. The levels of Bb-specific IgG and IgG1 in GAN-OMV group were higher than that of alum-OMV group. The levels of Bb-specific IgG2a in GAN-OMV group was significantly higher than the alum-OMV group.
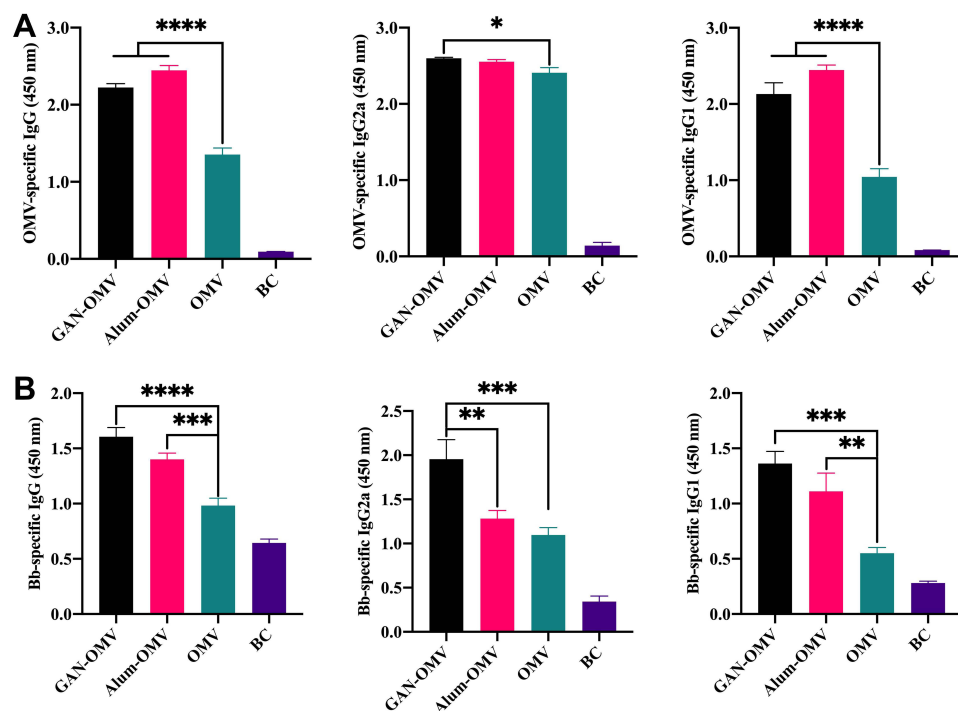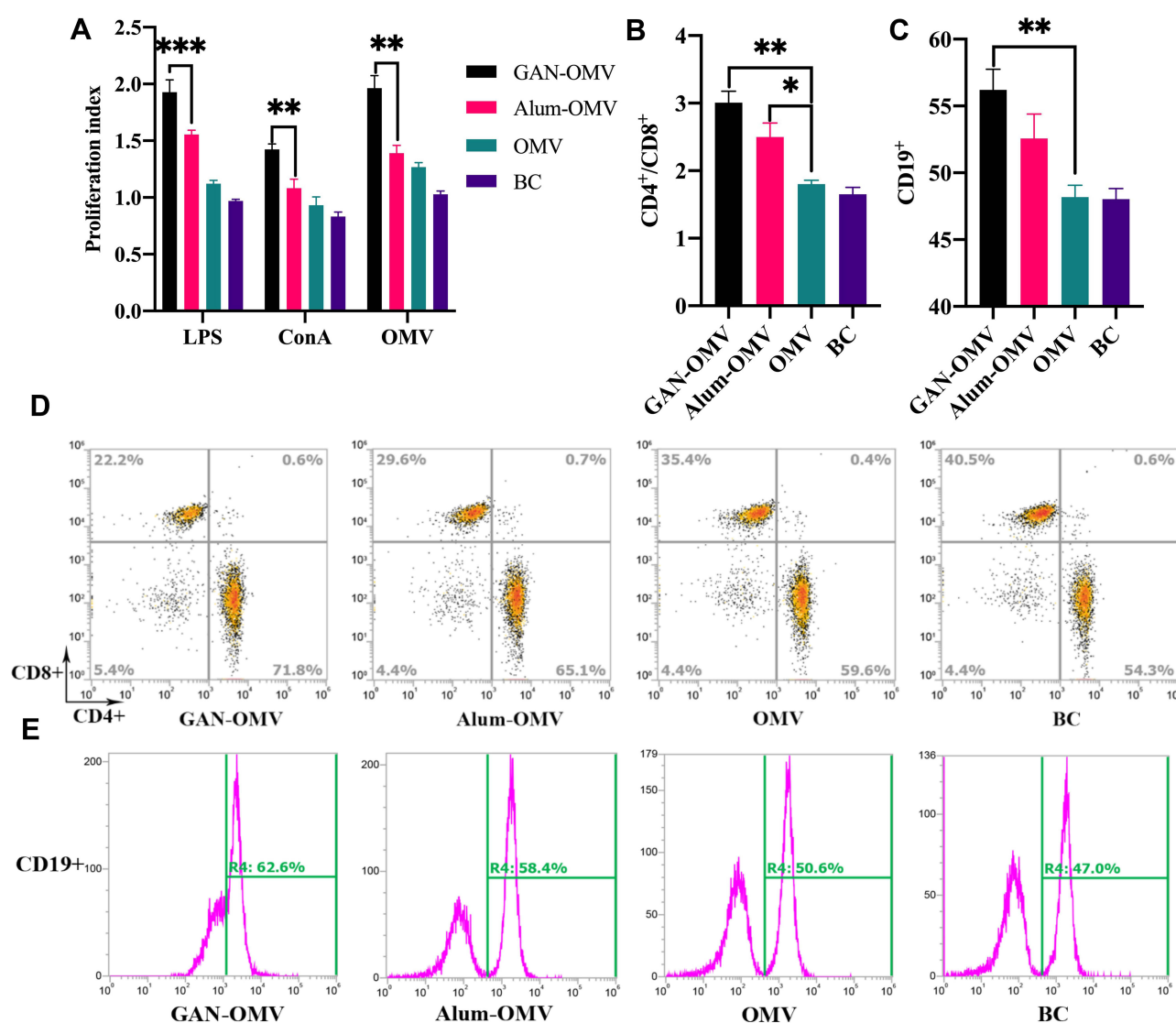

Figure 6 Antigen-specific antibodies produced by GAN-OMV-immunized mice. Mice (n=6) received either GAN-OMV, alum-OMV, OMV, or PBS (BC) in three doses in 7-day interval. Serum was collected 4 weeks after the last immunization. (**A**) OMV-specific and (**B**) Bb-specific IgG, IgG1, and IgG2a were analyzed by ELISA. *$P<0.05$, **$P<0.01$, ***$P<0.001$, ****$P<0.0001$.

GAN-OMV Increased Cell Proliferation and Cytokine Production

Lymphocytes are responsible for adaptive immune response. After the third immunization, immunized and non-immunized mice were sacrificed on day 42 in aseptic conditions, and spleens were collected to assess the proliferation and differentiation of B and T lymphocyte subsets.

Splenic lymphocytes from immunized and non-immunized mice were stimulated with LPS, ConA, and OMV, respectively. GAN-OMV-immunized mice showed significantly higher lymphocyte proliferation than that of both alum-OMV and single OMV (Figure 7A). In the present study, lymphocyte differentiation and activation were assessed by measuring the levels of the markers (CD3, CD4, CD8, and CD19) on the surface of effector lymphocyte cells by flow cytometry.[27] The ratio of CD4+/CD8+ T cells was compared after CD3+ T cells were gated. A significantly higher CD4+/CD8+ ratio was observed in the splenic lymphocytes of mice vaccinated with GAN-OMV than those vaccinated with alum-OMV and single OMV (Figure 7B–E). These results also showed that the frequency of CD19+ B cell was significantly higher in the GAN-OMV immunized group than that of alum-OMV and OMV, indicating that GAN-OMV enhances the activation of the B cell activation.

Figure 7 Splenocyte proliferation and differentiation of GAN-OMV-immunized mice. Mice (n=6) received either GAN-OMV, alum-OMV, OMV, or PBS (BC) in three doses in a 7-days interval. Splenocytes were collected after 4 weeks and stimulated with either LPS, ConA, or OMV. (**A**) The proliferation of LPS/ConA/OMV-stimulated lymphocytes from the spleen of immunized mice was measured by CCK-8 assay. (**B**) The quantitative data of (**B**) CD4+/CD8+ and (**C**) CD19+ splenocytes. Following CD3+ splenocyte gating, (**D**) CD4+ or CD8+ cells were analyzed. (**E**) CD19+ splenocytes were also analyzed by flow cytometry. *P<0.05, **P<0.01, ***P<0.001.
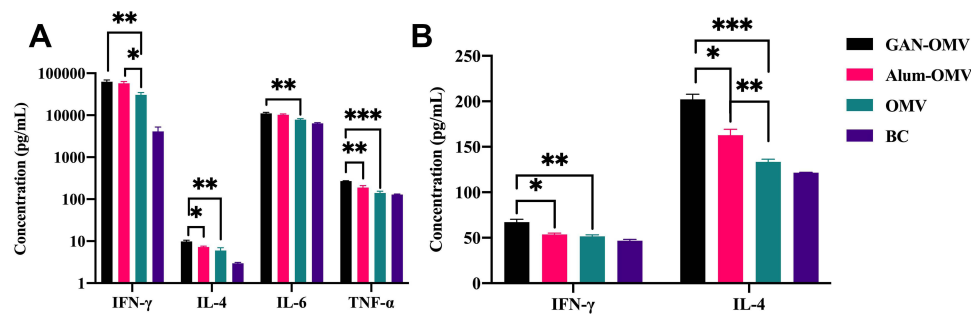
Figure 8 Cytokine production by splenocytes and in the serum of immunized mice. (**A**) Splenocytes were collected from immunized mice, and ELISA analyzed the Th1/Th2/Th17 cytokine production in the cell culture supernatant. (**B**) IFN-γ and IL-4 production in the serum of immunized mice was measured by ELISA. The data are reported as mean±SE (n=6). A statistically significant difference was determined between the groups by one-way ANOVA. *$P<0.05$; **$P<0.01$; ***$P<0.001$.

Quantitative ELISA was used to measure the level of Th1 (IFN-γ), Th2 (IL-4), and Th17 (IL-6 and TNF-α) cytokines in OMV-activated splenocytes isolated from immunized mice compared to the negative controls. Both GAN-OMV and alum-OMV enhance Th1, Th2, and Th17 cytokine secretion, significantly higher than the single OMV group. Compared to alum-OMV, there is only a slight increase in IFN-γ and IL-6 secretion in the GAN-OMV group, while IL-4 and TNF-α were significantly increased in the GAN-OMV-immunized group compared to the alum-OMV group (Figure 8A).

The serum levels of IL-4 and IFN-γ in immunized mice were also tested. Figure 8B shows significantly higher levels of both cytokines in the GAN-OMV immunized mice serum than in the alum-OMV and OMV groups.

GAN-OMV Prevented Secondary Infection

To confirm the protective efficacy of our GAN-OMV vaccine, the bactericidal activity of the serum from immunized mice was tested. Compared to the serum of the unimmunized group, that from all the immunized mice showed a significantly higher bactericidal activity. Also, the serum of GAN-OMV-immunized mice showed a significantly higher bactericidal activity compared to the alum-OMV and OMV groups (Figure 9A). These results indicated that GAN-OMV improves serum bactericidal activity.

Decreased colonization of bacteria in host tissues and organs facilitates the evaluation of the protective effect of vaccines. The number of bacteria invading the lung in the immunized mice after Bb challenge was estimated. In the lungs of GAN-OMV immunized mice, only a few Bb bacteria could be detected, which was significantly lower than that in the alum-OMV and OMV groups. Simultaneously, naïve mice were heavily colonized after Bb challenge (Figure 9B).
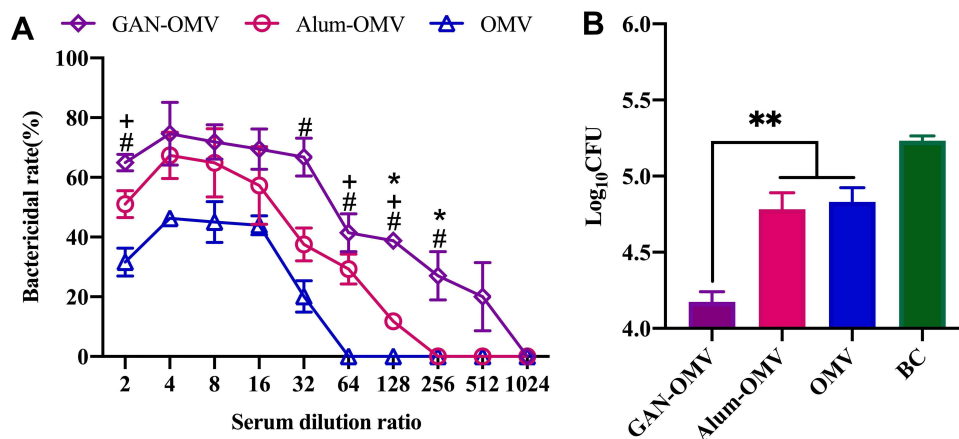
Figure 9 Reinfection prevention efficacy of GAN-OMV. Four weeks after the last vaccination, the serum of the immunized mice was collected, and the mice were subjected to Bb challenge ($6.5×10^6$ CFU/mouse). (**A**) Bactericidal activity of the serum collected from immunized mice. (**B**) Number of Bb bacteria colonized in the lungs of immunized and naïve mice. *$P<0.05$; **$P<0.01$ for GAN-OMV vs alum-OMV. #$P<0.05$ for GAN-OMV vs OMV group. +$P<0.05$ for alum-OMV vs OMV group.

Overall, these data indicated that immunization with GAN-OMV induces a significant protective immune response against Bb infection.

Discussion

Vaccination is regarded as the most cost-effective method for preventing infectious diseases. Among the various strategies of vaccination, OMV showed a promising prospect.[28] Collecting directly from the bacterial outer membranes of the bacteria, OMV shared a great similarity in biochemical profiles with their parent cells. OMV-based Group B meningococcal vaccine MeNZB (Besero[TM]) was successful in limiting the incidence and mortality of meningitis in New Zealand.[29] Also, OMV-expressing antigens from influenza virus, *Pneumococcus, Chlamydia*, or Group A and B *Streptococcus* stimulate the body to produce specific antibodies against these pathogenic microorganisms.[30–33]

According to the clinical results, OMV has low structural stability, which is not favorable to elicit the vaccine effect.[28] The current results also showed that the average size of OMV from Bb increased rapidly when stored at 4°C ([Figure S3](#)). A stable structure contributes to an effective uptake by APCs, resulting in an enhanced antigen-specific immune response. To address this challenge, a nano vaccine with integrated OMV and GA was developed.

Owing to the hydrophobic and hydrophilic moieties, GA has an amphiphilic nature and self-assembly behavior in water. GAN retains the immunomodulatory efficacy of GA and resolves the problem of poor water solubility. Recently, the cell membrane biomimetic NPs have attracted increasing attention,[34] and OMV coating synthetic nanoparticles holds great promise for developing effective antibacterial vaccines, including some resistant bacteria.[28,35] Based on this technique, the OMV was employed to coat self-assembled GAN through an extrusion process. The size of GAN-OMV was between 10 and 300 nm, with an average size of 130.43 nm. During the same time, the size of GAN-OMV hardly showed any changes, while OMV increased by 14 nm simultaneously ([Figure S3](#)), indicating that the structural stability of GAN-OMV improved significantly as compared to OMV.

Then, the in vitro immunological function on macrophages was compared. As vital immune cells in the innate system, macrophages play an essential role in defense against microbial infections and immunological diseases. Also, the macrophages can remove the external invaders via secretory proinflammatory cytokines, such as TNF-α and IL-6. Thus, macrophages have been considered a classic cell model to evaluate the activity of immunomodulatory factors.[36] GAN-OMV promoted macrophage proliferation and significantly increased its cytokine secretion, which is crucial for mediating the subsequent adaptive immune response. Moreover, GAN-OMV stimulated BMDMs to exhibit M1 polarization. Reportedly, M1 macrophages showed high antigen presentation and promoted Th1 differentiation of lymphocytes that produce proinflammatory cytokines in response to intracellular pathogens. M1 macrophages also inhibit iron export, thereby restricting the availability of microenvironmental iron that aids bacterial expansion, thereby preventing the infection.[37] Our results further indicated that through micropinocytosis-dependent and clathrin-mediated endocytotic pathways, GAN-OMV internalizes into the macrophages and is accumulated in the lysosomes in the cytoplasm.

Based on the in vitro data, the ability of GAN-OMV to induce a strong specific immune response against Bb upon subcutaneous immunization was further investigated. The antibodies produced during vaccination contributed to protective immunity.[38] The level of both OMV-specific and Bb-specific antibodies induced by GAN-OMV was significantly improved compared to single OMV. When comparing with the alum-OMV, Bb-specific antibody induced by GAN-OMV was higher, which is a direct indication of a protective immune response against pathogenic bacteria.

Lymphocyte proliferation is the first step in an immune response to create effector lymphocytes, essential for antigen elimination. T lymphocytes are primarily responsible for mounting a cell-mediated immune response, while B lymphocytes for a humoral immune response.[39] A significantly higher proliferation level was observed in the mice immunized with GAN-OMV, and the proliferation index of LPS-, ConA-, and OMV-stimulated splenic lymphocytes showed a significant increase. Also, the ratio of CD4+/CD8+ T cells and CD19+ B cells was significantly increased in the GAN-OMV group compared to the OMV group, while compared to the alum-OMV group, the increase was not significant. Thus, the activation of splenic lymphocytes by vaccination is necessary for initiating humoral and cellular immune responses.[27]

Cytokines secreted by immune cells, especially lymphocytes, play a critical role in initiating and regulating immune responses that are imperative for the elimination of infected cells and pathogens.[40] The cytokine secretion was assessed

subsequently, and as expected, a significantly higher level of Th1 (IFN-γ), Th2 (IL-4), and Th17 (IL-6 and TNF-α) cytokines were secreted by splenic lymphocytes from GAN-OMV immunized mice. The cytokine levels in the serum of the GAN-OMV group were also significantly higher than that of both alum-OMV and OMV group. Thus, it could be deduced that repeated subcutaneous injections of our nanoformulated OMV-based vaccine exert a potent mixed Th1/Th2/Th17 immune response, which is one of the major features of protective immune response.[41]

In addition to the immunological efficiency in vivo, GAN-OMV also controls Bb reinfection. Serum from GAN-OMV-immunized mice exhibited significantly higher bactericidal activity than other groups, which laid a foundation for controlling Bb reinfection. Also, a significantly decreased bacterial colonization was observed in the lung from GAN-OMV-immunized mice after Bb challenge, which further confirmed the protective efficacy of our nanoformulated OMV-based vaccine in controlling pathogen reinfection.

Conclusion

In summary, GAN reinforced OMV structural stability, which in turn stimulated the Th1/Th2/Th17 immune responses. GAN-OMV is effectively internalized into macrophage through micropinocytosis-dependent and clathrin-mediated endocytotic pathways, resulting in increased cell proliferation and cytokine secretion. Moreover, GAN-OMV-stimulated macrophages showed M1 polarization, which facilitated immune responses against bacterial infection. When administered subcutaneously, GAN-OMV remarkably enhances the Bb-specific IgG and Th1, Th2, and Th17 cytokines, contributing to a robust protective immune response against Bb; GAN-OMV also prevented Bb reinfection. Taken together, this study demonstrated a significant potential of nano-formulated GAN-OMV as a vaccine platform that can elicit a strong specific immune response against the microbial pathogens.

Acknowledgment

Disclosure

The authors report no conflicts of interest concerning this article.

References

1. Li M, Zhou H, Yang C, et al. Bacterial outer membrane vesicles as a platform for biomedical applications: an update. *J Control Release*. 2020;323:253–268. doi:10.1016/j.jconrel.2020.04.031

2. De Jonge EF, Balhuizen MD, van Boxtel R, Wu J, Haagsman HP, Tommassen J. Heat shock enhances outer-membrane vesicle release in Bordetella spp. *Curr Res Microb Sci*. 2021;2:100009.

3. Ojima Y, Sawabe T, Konami K, Azuma M. Construction of hypervesiculation Escherichia coli strains and application for secretory protein production. *Biotechnol Bioeng*. 2020;117(3):701–709. doi:10.1002/bit.27239

4. Micoli F, MacLennan CA. Outer membrane vesicle vaccines. *Semin Immunol*. 2020;50:101433. doi:10.1016/j.smim.2020.101433

5. Chen HY, Deng J, Wang Y, Wu CQ, Li X, Dai HW. Hybrid cell membrane-coated nanoparticles: a multifunctional biomimetic platform for cancer diagnosis and therapy. *Acta Biomater*. 2020;112:1–13. doi:10.1016/j.actbio.2020.05.028

6. Balmert SC, Little SR. Biomimetic delivery with micro- and nanoparticles. *Adv Mater*. 2012;24(28):3757–3778. doi:10.1002/adma.201200224

7. Wang F, Chen G, Zhao Y. Biomimetic nanoparticles as universal influenza vaccine. *Smart Mater Med*. 2020;1:21–23. doi:10.1016/j.smaim.2020.03.001

8. Bernela M, Ahuja M, Thakur R. Enhancement of anti-inflammatory activity of glycyrrhizic acid by encapsulation in chitosan-katira gum nanoparticles. *Eur J Pharm Biopharm*. 2016;105:141–147. doi:10.1016/j.ejpb.2016.06.003

9. Juin SK, Ghosh S, Majumdar S. Glycyrrhizic acid facilitates anti-tumor immunity by attenuating Tregs and MDSCs: an immunotherapeutic approach. *Int Immunopharmacol*. 2020;88:106932. doi:10.1016/j.intimp.2020.106932

10. Matsui S, Matsumoto H, Sonoda Y, et al. Glycyrrhizin and related compounds down-regulate production of inflammatory chemokines IL-8 and eotaxin 1 in a human lung fibroblast cell line. *Int Immunopharmacol*. 2004;4(13):1633–1644. doi:10.1016/j.intimp.2004.07.023

11. Sui X, Wei W, Yang L, et al. Preparation, characterization and in vivo assessment of the bioavailability of glycyrrhizic acid microparticles by supercritical anti-solvent process. *Int J Pharm*. 2012;423(2):471–479. doi:10.1016/j.ijpharm.2011.12.007

12. Saha A, Adamcik J, Bolisetty S, Handschin S, Mezzenga R. Fibrillar networks of glycyrrhizic acid for hybrid nanomaterials with catalytic features. *Angew Chem*. 2015;54(18):5408–5412. doi:10.1002/anie.201411875

13. França MT, Marcos TM, Costa PF, Gerola AP, Stulzer HK. The role of glycyrrhizic acid in colloidal phenomena of supersaturation drug delivery systems containing the antifungal drug griseofulvin. *J Mol Liq*. 2020;301:112336. doi:10.1016/j.molliq.2019.112336

14. Belhart K, Gutierrez MP, Zacca F, et al. Bordetella bronchiseptica diguanylate cyclase BdcA regulates motility and is important for the establishment of respiratory infection in mice. *J Bacteriol*. 2019;201(17):e00011–e00019.

15. Gupta S, Goyal P, Mattana J. Bordetella bronchiseptica pneumonia a thread in the diagnosis of human immunodeficiency virus infection. *IDCases*. 2019;15:e00509. doi:10.1016/j.idcr.2019.e00509

16. Li N, Yee H, Chenwen X, et al. Preparation of outer membrane vesicles from rabbit Bordetella bronchiseptica and their protein composition analysis. J Zhejiang Univ. 2021;47(2):251–260.

17. Huang Y, Nan L, Xiao C, et al. Optimum preparation method for self-assembled pegylation nano-adjuvant based on Rehmannia glutinosa polysaccharide and its immunological effect on macrophages. *Int J Nanomed*. 2019;14:9361–9375. doi:10.2147/IJN.S221398

18. Wei T, Chen C, Liu J, et al. Anticancer drug nanomicelles formed by self-assembling amphiphilic dendrimer to combat cancer drug resistance. *PNAS*. 2015;112(10):2978–2983. doi:10.1073/pnas.1418494112

19. Huang Y, Nan L, Xiao C, et al. PEGylated nano-Rehmannia glutinosa polysaccharide induces potent adaptive immunity against Bordetella bronchiseptica. *Int J Biol Macromol*. 2021;168:507–517. doi:10.1016/j.ijbiomac.2020.12.044

20. Jiang S, Yin H, Li R, Shi W, Mou J, Yang J. The activation effects of fucoidan from sea cucumber Stichopus chloronotus on RAW264.7 cells via TLR2/4-NF-κB pathway and its structure-activity relationship. *Carbohyd Polym*. 2021;270:118353. doi:10.1016/j.carbpol.2021.118353

21. Huang L, Shen M, Morris GA, Xie J. Sulfated polysaccharides: immunomodulation and signaling mechanisms. *Trends Food Sci Tech*. 2019;92:1–11. doi:10.1016/j.tifs.2019.08.008

22. Zhong X, Zhang Y, Tan L, et al. An aluminum adjuvant-integrated nano-MOF as antigen delivery system to induce strong humoral and cellular immune responses. *J Control Release*. 2019;300:81–92. doi:10.1016/j.jconrel.2019.02.035

23. Li H, Somiya M, Kuroda S. Enhancing antibody-dependent cellular phagocytosis by Re-education of tumor-associated macrophages with resiquimod-encapsulated liposomes. *Biomaterials*. 2021;268:120601. doi:10.1016/j.biomaterials.2020.120601

24. Xu L, Xie X, Luo Y. The role of macrophage in regulating tumour microenvironment and the strategies for reprogramming tumour-associated macrophages in antitumour therapy. *Eur J Cell Biol*. 2021;100(2):151153. doi:10.1016/j.ejcb.2021.151153

25. Masuda J, Shigehiro T, Matsumoto T, et al. Cytokine expression and macrophage localization in xenograft and allograft tumor models stimulated with lipopolysaccharide. *Int J Mol Sci*. 2018;19:4. doi:10.3390/ijms19041261

26. Koshy ST, Mooney DJ. Biomaterials for enhancing anti-cancer immunity. *Curr Opin Biotechnol*. 2016;40:1–8. doi:10.1016/j.copbio.2016.02.001

27. Liu Z, Yu L, Gu P, et al. Preparation of lentinan-calcium carbonate microspheres and their application as vaccine adjuvants. *Carbohydr Polym*. 2020;245:116520. doi:10.1016/j.carbpol.2020.116520

28. Wu G, Ji H, Guo X, et al. Nanoparticle reinforced bacterial outer-membrane vesicles effectively prevent fatal infection of carbapenem-resistant Klebsiella pneumonia. *Nanomedicine*. 2020;24:102148.

29. Petousis-Harris H, Paynter J, Morgan J, et al. Effectiveness of a group B outer membrane vesicle meningococcal vaccine against gonorrhoea in New Zealand: a retrospective case-control study. *Lancet*. 2017;390(10102):1603–1620. doi:10.1016/S0140-6736(17)31449-6

30. Rappazzo CG, Watkins HC, Guarino CM, et al. Recombinant M2e outer membrane vesicle vaccines protect against lethal influenza A challenge in BALB/c mice. *Vaccine*. 2016;34(10):1252–1258. doi:10.1016/j.vaccine.2016.01.028

31. Bartolini E, Ianni E, Frigimelica E, et al. Recombinant outer membrane vesicles carrying Chlamydia muridarum HtrA induce antibodies that neutralize chlamydial infection in vitro. *J Extracell Vesicles*. 2013;2(1):20181.

32. Fantappie L, de Santis M, Chiarot E, et al. Antibody-mediated immunity induced by engineered Escherichia coli OMVs carrying heterologous antigens in their lumen. *J Extracell Vesicles*. 2014;3(1):24015.

33. Kuipers K, Daleke-Schermerhorn MH, Jong WS, et al. Salmonella outer membrane vesicles displaying high densities of pneumococcal antigen at the surface offer protection against colonization. *Vaccine*. 2015;33(17):2022–2029. doi:10.1016/j.vaccine.2015.03.010

34. Fang RH, Kroll AV, Gao W, Zhang L. Cell membrane coating nanotechnology. *Adv Mater*. 2018;30(23):e1706759. doi:10.1002/adma.201706759

35. Gao W, Fang RH, Thamphiwatana S, et al. Modulating antibacterial immunity via bacterial membrane-coated nanoparticles. *Nano Lett*. 2015;15(2):1403–1409. doi:10.1021/nl504798g

36. Huang Z, Zeng YJ, Chen X, et al. A novel polysaccharide from the roots of Millettia Speciosa Champ: preparation, structural characterization and immunomodulatory activity. *Int J Biol Macromol*. 2020;145:547–557. doi:10.1016/j.ijbiomac.2019.12.166

37. Sridharan R, Cameron AR, Kelly DJ, Kearney CJ, O'Brien FJ. Biomaterial based modulation of macrophage polarization: a review and suggested design principles. *Mater Today*. 2015;18(6):313–325.

38. Sahu R, Dixit S, Verma R, et al. A nanovaccine formulation of Chlamydia recombinant MOMP encapsulated in PLGA 85:15 nanoparticles augments CD4(+) effector (CD44(high) CD62L(low)) and memory (CD44(high) CD62L(high)) T-cells in immunized mice. *Nanomedicine*. 2020;29:102257. doi:10.1016/j.nano.2020.102257

39. Levin M, Jasperse L, Desforges JP, et al. Methyl mercury (MeHg) in vitro exposure alters mitogen-induced lymphocyte proliferation and cytokine expression in steller sea lion (Eumetopias jubatus) pups. *Sci Total Environ*. 2020;725:138308. doi:10.1016/j.scitotenv.2020.138308

40. Gu P, Wusiman A, Wang S, et al. Polyethylenimine-coated PLGA nanoparticles-encapsulated Angelica sinensis polysaccharide as an adjuvant to enhance immune responses. *Carbohydr Polym*. 2019;223:115128. doi:10.1016/j.carbpol.2019.115128

41. Raeven RHM, Rockx-Brouwer D, Kanojia G, et al. Intranasal immunization with outer membrane vesicle pertussis vaccine confers broad protection through mucosal IgA and Th17 responses. *Sci Rep*. 2020;10(1):7396. doi:10.1038/s41598-020-63998-2